ISSN : 2231-0711

Mustafa S. Hussein et al | International Journal of Computer Science Engineering and Technology(IJCSET) | November 2014 | Vol 4, Issue 11,326-332

Parametric Performance Evaluation of a Printed Pixel Monopole Antenna

Mustafa S. Hussein[#1], Lubab A. Salman[#2]

[#]*Department of Electronic and Communications Engineering, Al-Nahrain University*
PO Box 64040, Baghdad, Iraq

***Abstract*— A pixel monopole antenna could be recognized as a broadband reconfigurable antenna with the capability of multi-objective real-time optimization to meet the specific needs of a particular application or operating conditions. It allows a wide range of reconfigurability options as it enables accurate simultaneous control of its spatial and frequency domains characteristics in real time by allowing a large number of functionality states. This operational versatility, however, is limited to the extent made possible by the device's fixed design parameters. These include the substrate's material and height, the size of the individual pixel elements and the spacing between them which determines the size of the overall radiating aperture, and the feed mechanism and the associated broadband impedance matching parameters. The impact of these parameters on the performance of a 3×3 fully interconnected planar pixel monopole antenna is investigated in this paper.**

***Keywords*— parametric, reconfigurable, planar, printed, pixel, monopole, antenna.**

I. INTRODUCTION

Pixel antennas are either planar [1], [2] or conformal [3], [4] radiating structures, with reconfigurable apertures promising of unprecedented real-time control [5], [6] of their spatial and frequency domains features [7]-[9]. They are making it possible by incorporating a reconfigurable grid of strongly-coupled small radiating elements (pixels) as their main radiating aperture. Pixels, which may take on different shapes [10]-[12], are switched in or out of the aperture in response to the variable requirements imposed by the antenna's operating conditions. In this context, pixel antennas have also been referred to as software-defined radiating apertures [13]-[16]. Different approaches have been proposed in the literature to allow for this functionality.

In one approach, a pixel antenna is made of a grid of pixels; each one is attached to the top of a piston whose one of its two possible positions is determined by a computer code through a suitable interface in a way to select one of pre-set configuration states [14]-[17]. In that way the radiation aperture could be reconfigured instantaneously in whatever shape whose salient radiation and electrical features are desired. Despite the apparent reconfiguration flexibility and accuracy of this approach, it comes about at the cost of increased complexity which makes it unattractive in terms of scalability and efficiency. A trade-off is brought on by another approach whereby a grid of closely-spaced printed pixel elements, interconnected through controllable electronic switches, is employed to constitute the reconfigurable aperture. In this approach, the pixel elements are not switched on or off the aperture, rather they would always be present as part of either driven or parasitic sections of the aperture [7], [8], [18]-[23]. This of course would not make it possible to completely reshape the antenna's physical radiating aperture; rather, they would allow redirecting the flow if its surface currents by means of reshaping its driven and parasitic sectors. Although at the cost of reduced restructuring flexibility, this latter approach brings forth increased scalability and efficiency by relying mainly on electronic rather than mechanical switches. This of course does not exclude the utilization of RF-MEMS switches whose performance is comparable or superior to semiconductor switches in some situations. In a rather third approach, a pixel antenna is implemented relying on microfluidic technology [Rodrigo 2013-PhD]. In this technique pixel elements are switched on or off by electrostatically controlling the flow of a liquid metal to fill or evacuate a polymer-made container in the radiating aperture. Although this approach allows complete aperture reconfigurability, its technology is rather at its infancy and suffers like with the first approach from an inherent increased complexity.

Despite the underlying implementation technology, pixel antenna design methodologies aim at achieving one of following performance goals and reconfiguration strategies: narrowband or broadband operation with single or multi-parameter reconfiguration capability. Where desired, narrowband performance with single or multi-parameter reconfigurability could be obtained by incorporating a pixelated reconfigurable radiating aperture backed by a ground plane. This structure is identified as microstrip pixel antenna. On the other hand, a broadband operation with single or multi-parameter reconfigurability could be achieved by the implementation of a pixelated dipole or monopole radiating aperture. In either case it would be of much use to be able to quantitatively identify the impact of the fixed design parameters on the overall performance of the device. To the extent of the author's knowledge, this issue has only been qualitatively and implicitly addressed in the open literature and the apparent need for a quantitative explicit treatment had been behind the inauguration of this study.

In the quest for that aim we are going to address the impact of the fixed design parameters of a planar pixel monopole antenna on its performance. The investigated design incorporates a 3×3 grid of strongly-coupled square pixel elements as the radiating aperture fed from a 50-Ω microstrip transmission line. All of the pixels are assumed to be permanently electrically connected to each other through metallic connection tabs. Although this might limit the usability of the obtained results, it would alternatively

allow studying the impact of the width of the connection tabs on the performance of the device in the fully-connected case. This study has been conducted through extensive full-wave simulation runs using Momentum® in the Advanced Design System (ADS) 2011 from Agilent®.

The rest of the paper is organized in two parts mainly. Section II presents parametric performance analysis of a conventional square-patch monopole antenna to serve as a reference model and benchmark for subsequent pixel antenna analysis. The parameters considered there include its patch length, permittivity, and substrate height and their impact on its frequency response, radiation pattern, and efficiency. Section III on the other hand presents the performance analysis of the pixel antenna under investigation and wherein the following parameters are considered: pixel-to-pixel spacing, pixel size, and the width of pixel-to-pixel connection tabs. Finally, concluding remarks and suggestions for future extension of this work are presented in Section IV.

II. Reference Monopole Antenna

Fig. 1 shows the geometry of square-patch reference monopole antenna situated in the *xy*-plane. It incorporates a 1.6 mm thick FR-4 substrate with a relative permittivity $\varepsilon_r = 4.6$ and a loss tangent of 0.01 at 1 GHz. On one side of the substrate a square radiating patch is printed with a side-length PL = 14 mm. The patch is fed from a 50-Ω microstrip line whose width is 2.9 mm printed on the same side of the substrate. The feed line is backed by a rectangular ground plane with dimensions 9.2 mm × 19.9 mm on the other side of the substrate. Matching between the feed line and the radiating patch is controlled by the size of the gap extending from the upper edge of the ground plane to the lower edge of the radiating patch. This gap is denoted GG and is set to 1.2 mm.

The reflection coefficient in dB of the reference square monopole antenna is shown in Fig. 2 as a function of frequency. It can be seen that the antenna has a broad -10 dB bandwidth of about 4.5 GHz starting at 3.3 GHz. The E (*yz*)-plane and H (*xz*)-plane radiation gain patterns evaluated at 4.2 GHz are shown in Fig. 3. It can be seen that they are slightly tilted in compliance with the inherent asymmetry of the antenna structure with respect to both planes. The two notches in the H-plane pattern of Fig. 3(b), which should otherwise be omnidirectional, is due to the fact that in Momentum® of ADS 2011 from Agilent® an infinite substrate is assumed and the surface waves excited in its direction are not included in the calculation of the far field radiation [24].

In the following subsections, the variation of the patch side-length, the substrate's relative permittivity, and the substrate's height, parameters and its impact on the antenna performance is going to be investigated thoroughly. A similar study have already been conducted by Panda and Kshetrimayum [25] on a rectangular monopole antenna with a microstrip feed line. Our study of the square patch monopole antenna considered here is included both for the sake of completeness and as a comparable reference benchmark using the same simulation tool used next for the analysis of the pixel antenna.

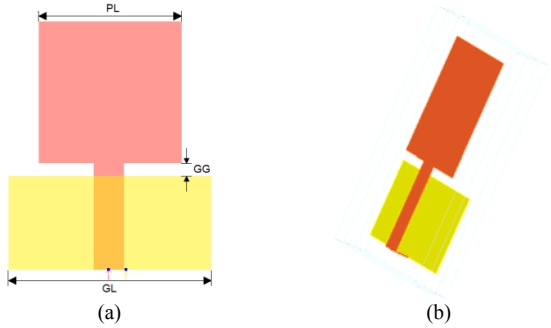

(a) (b)

Fig. 1 The reference square-patch monopole antenna. (a) A two-dimensional view with some geometrical parameters. (b) A three-dimensional view.

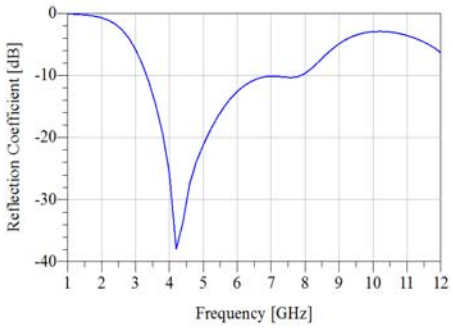

Fig. 2 The reflection coefficient of the reference square-patch monopole antenna with PL=14 mm, GG=1.2 mm. and GL=19.9 mm.

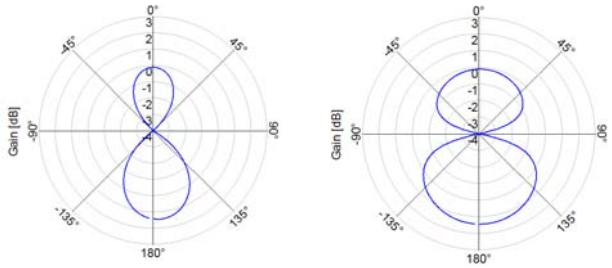

(a) (b)

Fig. 3 E-plane (a) and H-plane (b) radiation patterns for the reference monopole antenna at 4.2 GHz.

A. Patch Side-Length

It is well-known that the frequency response of the antenna is directly related to its electrical length which is ultimately determined by its physical length and the frequency of operation. According to Kumar and Ray [26] the lower cutoff frequency of the planer monopole antenna is approximately given by:

$$f_L = \frac{7.2}{(PL + \frac{PL}{2\pi} + GG) \times 0.1} \; GHz \qquad (1)$$

where PL and GG are measured in millimetres.

Here, PL is swept from 12 mm to 17 mm in 1 mm steps and the resultant variation in the reflection coefficient is shown in Fig. 4. Table I summarizes the results obtained regarding the beginning and end of the operating bandwidth. It can be seen that increasing PL has the effect

of slightly decreasing the lower cutoff frequency in compliance with Eq. 1. On the other hand, it is seen that varying PL is significantly affecting the upper cutoff frequency in an inverse manner causing the operating bandwidth to decrease as PL increases.

Fig. 5 shows the radiation pattern for two PL values. It can be seen they are only slightly affected by the variation in PL.

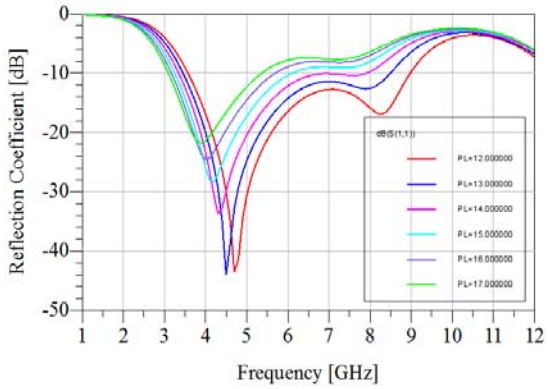

Fig. 4 The variation of the antenna reflection coefficient with the variation of the design parameter PL, with GG = 1.25 mm and ground size 9.2 × 19.8 mm.

TABLE I
SIMULATION RESULTS FOR DIFFERENT PATCH LENGTH (PL) VALUES FOR THE SQUARE-PATCH MONOPOLE ANTENNA SHOWN IN FIG. 1

PL (mm)	Lower cutoff frequency (GHz)	Upper cutoff frequency (GHz)	BW (GHz)
12	3.6	9	5.4
13	3.5	8.5	5
14	3.4	7.8	4.4
15	3.3	6.10	2.8
16	3.2	5.7	2.5
17	3.1	5.4	2.3

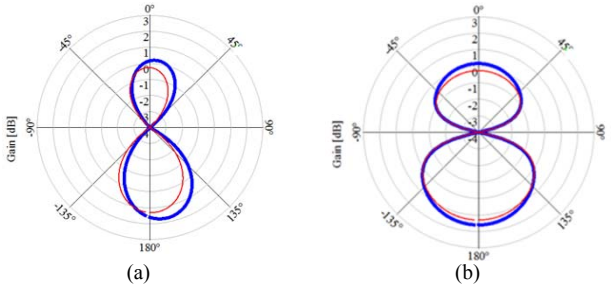

(a) (b)

Fig. 5 (a) E-plane and (b) H-plane radiation patterns of the square-patch monopole antenna operating at 4.2 GHz with PL = 12 mm (red line), and PL = 17 mm (blue line).

B. The Substrate's Relative Permittivity

Here the impact of the substrate's relative permittivity (ε_r) is investigated. Fig. 6 shows the reflection coefficient for different values of ε_r. It can be seen that the antenna bandwidth increases with the decrease of the dielectric constant. The variation of the more important antenna performance parameters with the variation of ε_r is summarized in Table II. It can be seen that the antenna directivity (D) increases as ε_r increases while its efficiency (η) decreases at higher rate with ε_r, eventually leading to an overall decrease in the antenna gain (G) with the increase in ε_r. Fig. 7 shows the realized gain for $\varepsilon_r = 2.7$ and $\varepsilon_r = 6$. It can be seen that a larger gain can be achieved when $\varepsilon_r = 2.7$ and that the gain decreases with the larger value of the dielectric constant. Fig. 8, on the other hand, reflects the fact that the antenna efficiency decreases almost linearly with the increase of ε_r.

TABLE II
SIMULATION RESULTS FOR DIFFERENT VALUES OF THE SUBSTRATE PERMITTIVITY E_R

ε_r	Lower cutoff frequency (GHz)	Upper cutoff frequency (GHz)	BW (GHz)	G (dBi)	D (dBi)	η
2.7	3.95	9.65	5.70	2.30	3.59	74%
3.5	3.69	8.56	4.87	2.07	3.93	65%
4.6	3.40	7.50	4.10	1.59	4.27	54%
6.0	3.12	6.00	2.88	1.00	4.58	44%

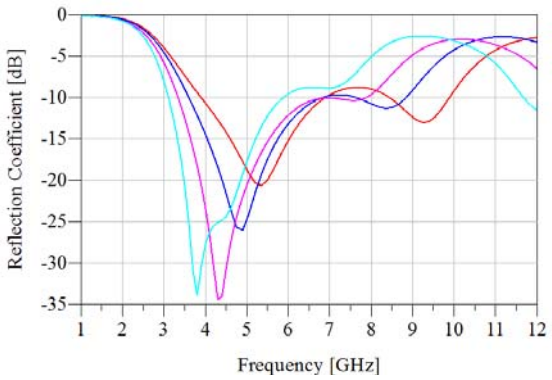

Fig. 6 Simulated reflection coefficient of the antenna corresponding to different (standard) ε_r variations $\varepsilon_r = 2.7$ (red line), $\varepsilon_r = 3.5$ (blue line), $\varepsilon_r = 4.6$ (pink line), $\varepsilon_r = 6$ (bluish_green).

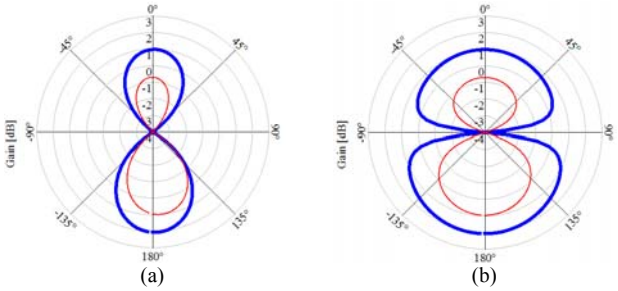

(a) (b)

Fig. 7 (a) E-plane and (b) H-plane radiation patterns of the square-patch monopole antenna operating at 4.2 GHz with $\varepsilon_r = 6$ (red line), and $\varepsilon_r = 2.7$ (blue line).

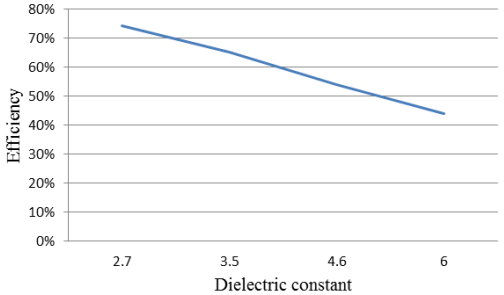

Fig. 8 The efficiency (η) of the square-patch monopole antenna as a function of the substrate's relative permittivity (ε_r).

C. *Substrate Height*

The reflection coefficient of the antenna is shown in Fig. 9 for different values of substrate height (h), and a summary of the corresponding variation of the main performance parameters is given in Table III below. It can be seen that the lower cutoff frequency is not very much affected by the increase in h, whereas it is evident that the upper cutoff frequency is greatly dependent on h. However, no specific trend in the variation of the latter can be observed leading to an unpredictable variation in the impedance bandwidth as a function of h. For example, a relatively large bandwidth is observed with substrate heights of 1.2 and 1.6 mm while much less bandwidth is observed for other height values.

Fig. 10 shows the realized gain for h = 2.4 mm and for h = 0.8 mm. It can be seen that the gain is inversely proportional to the substrate height, while directivity is directly proportional to it. This reflects the fact that the antenna efficiency is inversely proportional to the substrate height and it can be increased by about 30% by decreasing the substrate height from 2.4 mm to 0.8 mm as shown in Fig. 11.

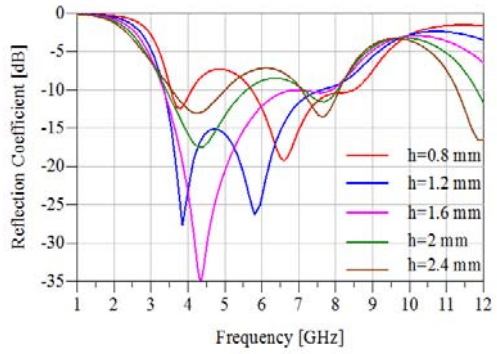

Fig. 9 Simulated reflection coefficient of the square-patch monopole antenna for different settings of the substrate height h.

TABLE III
SIMULATION RESULTS FOR DIFFERENT VALUES OF THE SUBSTRATE HEIGHT H

h (mm)	Lower cutoff frequency (GHz)	Upper cutoff frequency (GHz)	BW (GHz)	G (dBi)	D (dBi)	η
0.8	4.1	3.5	0.6	2.03	3.5	71%
1.2	3.4	7.6	4.2	1.81	3.89	61%
1.6	3.4	7.9	4.5	1.59	4.27	54%
2	3.4	5.5	2.1	1.38	4.64	47%
2.4	3.5	5	1.5	1.17	4.98	41%

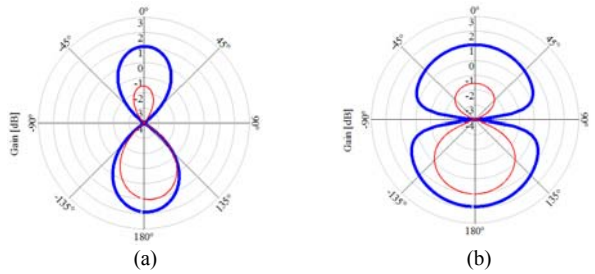

(a) (b)

Fig. 10 (a) E-plane and (b) H-plane radiation patterns of the square-patch monopole antenna operating at 4.2 GHz with h = 2.4 mm (red line), and h = 0.8 mm (blue line).

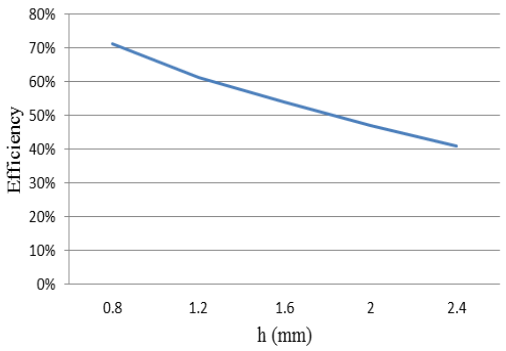

Fig. 11 Antenna efficiency (η) versus substrate height (h) in mm.

III. PIXEL MONOPOL ANTENNA

The geometry of a general fully-connected pixel monopole antenna is depicted in Fig. 12. The antenna structure consists of a printed grid of 3 × 3 square pixels of side-length w, separated from each other by P mm, with midway interconnecting tabs of width C. The distance from the upper edge of the ground plane to the lower edge of the pixel grid, GG is initially set to 1.2 mm. Three of the fixed design parameters and their impact on the antenna performance will be investigated in this section.

A. *Variable Pixel-to-Pixel Spacing with Fixed Pixel Size*

Varying the pixel-to-pixel spacing while keeping the pixel size fixed will vary the size of the whole radiating aperture. The pixel side-length is set to 4.67 mm (see Fig. 12) while the spacing P is varied from 0 mm (the reference model of Section II) to 2.5 mm which amounts to about 54% of the selected pixel side-length w.

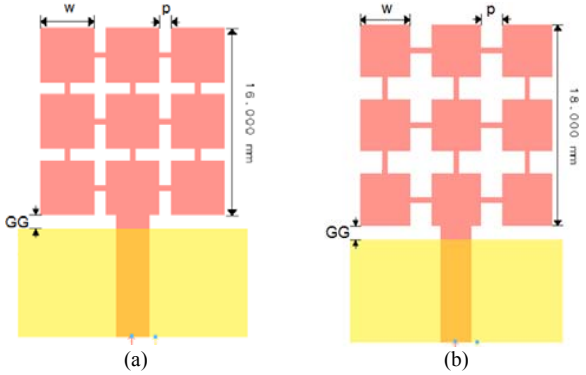

(a) (b)

Fig. 12 Varying pixel-to-pixel spacing while keeping pixel size fixed (w = 4.67 mm). (a) P = 1 mm, and (b) P = 2 mm. GG is set to 1.2 mm in both cases.

Fig. 13 shows the frequency response of the antenna in terms of its reflection coefficient for the indicated sweep of the parameter P. A summary showing the corresponding lower and upper cutoff frequencies and the associated bandwidth is given in Table IV. It can be clearly seen that increasing P causes the lower and upper cutoff frequencies to shift downward, but at slightly different rates leading eventually to a decrease in bandwidth.

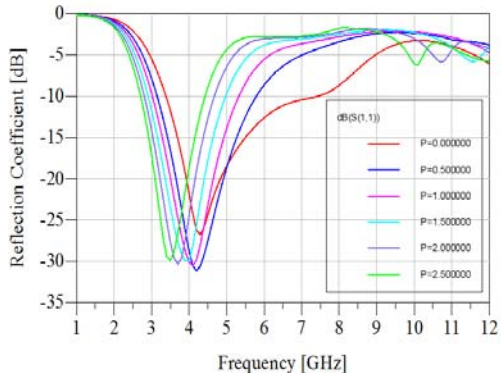

Fig. 13 Simulated reflection coefficient of the pixel antenna corresponding to variable gap width (P), when w = 4.67 mm and GG = 1.2 mm.

TABLE IV
SUMMARY OF THE FREQUENCY RESPONSE RESULTS CORRESPONDING TO VARIABLE PIXEL-TO-PIXEL SPACING (P) WHILE KEEPING OTHER PARAMETERS FIXED

P (mm)	Lower cutoff frequency (GHz)	Upper cutoff frequency (GHz)	BW (GHz)
0	3.4	7.6	4.2
0.5	3.1	5.8	2.7
1	3.0	5.3	2.3
1.5	2.9	5	2.1
2	2.8	4.7	1.9
2.5	2.7	4.4	1.7

Fig. 14 shows the realized gain for the two states P = 1 mm and P = 2 mm. It is clearly seen that the radiation pattern is only slightly changed with the pixel-to-pixel spacing variation.

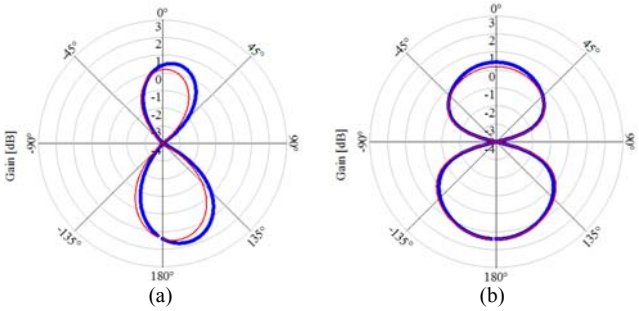

(a) (b)

Fig. 14 (a) E-plane and (b) H-plane radiation patterns (realized gain) of the pixel monopole antenna operating at 4.2 GHz, for P = 1 mm (red) and P = 2 mm (blue). w and GG are set to 4.67 mm and 1.2 mm, respectively.

B. *Variable Pixel-to-Pixel Spacing with Fixed Aperture Size*

Here, varying the pixel-to-pixel spacing will be accompanied by a reduction in pixel size in order to make the whole pixel grid fit into a fixed radiating aperture as shown in Fig. 15. The aperture side length is set to 14 mm and the spacing (S) is varied from zero (the reference model) to 2.5 mm (corresponding to about 83% of the pixel side length). The corresponding pixel width (w) then is given by

$$w = \frac{14 - 2 \times S}{3} \; mm \qquad (2)$$

Fig. 16 shows the reflection coefficient for different values of the spacing S. The lower and upper cutoff frequencies and the corresponding impedance bandwidth in each case is summarized in Table V. It can be seen that the lower cutoff frequency is almost unaffected by the varying spacing when the aperture size is kept fixed. On the other hand, the bandwidth is considerably reduced by the increase in S.

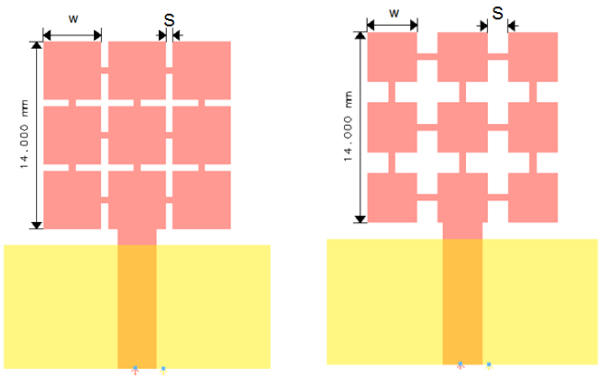

(a) (b)

Fig. 15 Variable pixel-to-pixel spacing with fixed radiating aperture. (a) w = 4.33 mm and S = 0.5 mm, and (b) w = 3 mm and S = 1.5 mm. GG is set to 1.2 mm in both cases.

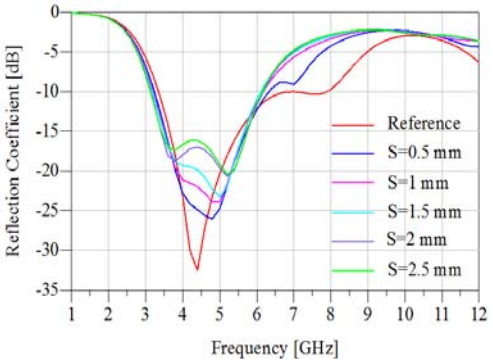

Fig. 16 Simulated reflection coefficient of the pixel antenna corresponding to the gaps width (S) and the corresponding pixel width (w) variations.

TABLE V
SUMMARY OF SIMULATION RESULTS FOR VARIABLE GAP WIDTH WITH FIXED RADIATIGN APERTURE AS SHOWN IN FIG. 18

S (mm)	Pixel width (w) (mm)	Lower cutoff frequency (GHz)	Upper cutoff frequency (GHz)	BW (GHz)
0	14	3.4	7.8	4.4
0.5	4.33	3.3	6.3	3.2
1	4	3.2	6.2	3
1.5	3.67	3.2	6.1	2.9
2	3.33	3.2	6.2	3
2.5	3	3.2	6.2	3

Fig. 17 shows the realized gain for the two cases for which S = 0.5 mm and S = 2.5 mm. It can be seen that the two cases have identical responses. Also, directivity, gain and efficiency remain unchanged for all of the spacing values considered.

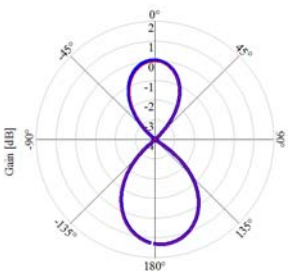

(a)

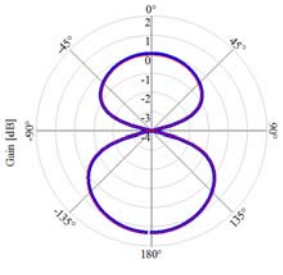

(b)

Fig. 17 (a) E-plane and (b) H-plane radiation patterns (realized gain) of the pixel monopole antenna operating at 4.2 GHz, with S = 0.5 mm and w = 4.33 mm (red) and S = 2.5 mm and w = 2.5 mm (blue).

C. Connection Tabs Width

The impact of the connection tabs width on the performance of the antenna is considered here. Although connectors are to be replaced by electronic switches in practice, some of them are sometimes left permanently connected if their presence has no significant impact on the desired antenna performance. In such a case, their width enters as a design parameter and its impact on the antenna performance needs to be evaluated. With the other parameters assumed fixed, the connection tabs width (C) is varied from 0.25 mm to 1 mm (or, in other words, from about 5% to 21% of the pixel side length) as shown in Fig. 18 below.

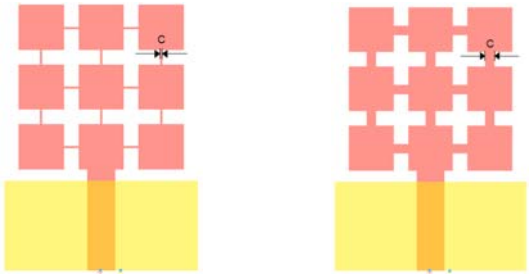

(a) (b)

Fig. 18 Variable connection tabs width with fixed pixel size and radiating aperture. (a) C = 0.25 mm. (b) C = 1 mm.

Fig. 19 shows the correlation coefficient for different C values. A summary of the results is also given in Table VI. It can be seen that the frequency response of the antenna is almost unaffected by the variation in C. Fig. 20 shows that the C has almost no effect on the radiation pattern of the antenna. Once again, directivity, gain, and efficiency remain unchanged in all cases.

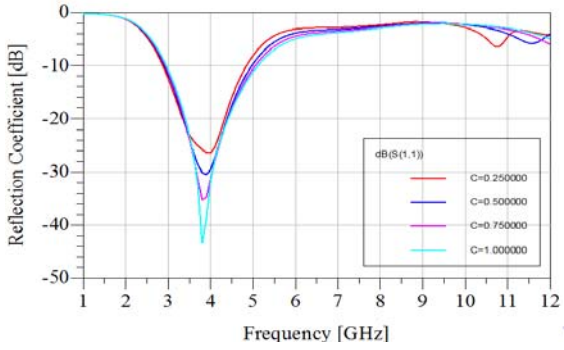

Fig. 19 Simulated reflection coefficient of the pixel antenna corresponding to the connections width (C) variations.

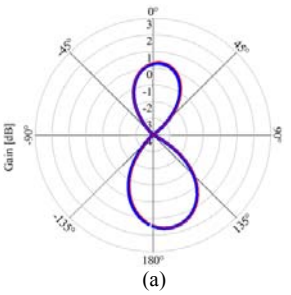

(a)

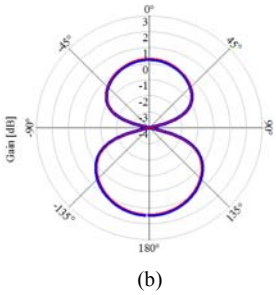

(b)

Fig. 22 (a) E-plane and (b) H-plane radiation patterns (realized gain) of the pixel monopole antenna operating at 4.2 GHz, with C = 0.25 mm (red) and C = 1 mm (blue).

TABLE VI
RESULTS OF SIMULATION FOR DIFFERENT CONNECTION TAB WIDTHS FOR THE STRUCTURE SHOWN IN FIG.

C (mm)	Lower cutoff frequency (GHz)	Upper cutoff frequency (GHz)	BW (GHz)
0.25	2.9	4.8	1.9
0.5	2.9	4.8	1.9
0.75	3	5	2
1	3	5.1	2.1

IV. CONCLUSIONS

A parametric study of a planar 3×3 pixel monopole antenna has been carried on to quantify the limitations imposed by a set of fixed design parameters on the performance of the antenna. The study has also included a conventional square-patch monopole antenna of comparable size to serve as a reference model. For the reference model, it has been seen that increasing the patch length has the effect of slightly decreasing the lower cutoff frequency while significantly decreasing the upper one. On the other hand, increasing the ground-to-patch distance leads to an increase in the impedance bandwidth. Furthermore, decreasing the substrate's permittivity and/or its height leads to a decrease in antenna directivity while rapidly increasing its efficiency, leading to an overall increase in the antenna gain.

For the pixel antenna under consideration, it has been seen that increasing the spacing between adjacent pixel elements while keeping their size fixed causes the lower and upper cutoff frequencies to shift downwards decreasing thereby the overall antenna bandwidth. However, increasing the spacing by reducing only the pixel size in an attempt to keep the overall radiating aperture unchanged has been found to be of negligible effect on the overall performance of the antenna. Similarly, it has been found that varying the width of the connection tabs joining adjacent pixels has leaves the antenna performance unaffected. This work could also be extended to investigate different pixel antenna structures and to include different switching conditions for the investigated structure.

REFERENCES

[1] J. C. Maloney, M. P. Kesler, and L. M. Lust, "Switched fragmented aperture antennas," *IEEE APS International Symposium*, vol. 11, 2000, pp. 310-313.

[2] L. N. Pringle, P. H. Harms, S. P. Blalock, G. N. Keisel, E. J. Kuster, P. G. Friederich, R. J. Prado, J. M. Morris, and G. S. Smith, "A reconfiturable aperture antenna based on switched links between

electrically small metallic patches," *IEEE Trans. Ant. Propagat.*, vol. 52, Jun 2004, pp. 1434-1445.

[3] N. Bishop, M. Ali, W. Baron, J. Miller, J. Tuss, and D. Zeppettella, "Aperture coupled MEMS reconfigurable pixel patch antenna for conformal load bearing antenna structures (CLAS)," *IEEE APSURSI 2014*, pp. 1091-1092.

[4] M. Ali, N. Bishop, W. Baron, B. Smyers, J. Tuss, and D. Zeppettella, "A MEMS reconfigurable pixel microstrip patch antenna for conformal load bearing antenna structures (CLAS) concept," *IEEE APSURSI 2014*, pp. 1093-1094.

[5] A. Muscat and J. A. Zammit, "An efficient algorithm for the control of reconfigurable pixel microstrip antennas," *IEEE Second ICACEME*, 2009, pp. 44-47.

[6] A. Muscat and J. A. Zammit, "A coupled random search-shape grammar algorithm for the control of reconfigurable pixel microstrip antennas," *IJASM*, vol. 3, 2010, pp. 186-197.

[7] D. Rodrigo and L. Jofre, "Frequency and Radiation Pattern Reconfigurability of a Multi-Size Pixel Antenna," *IEEE Trans. Ant. Propagat.*, vol. 60, May 2012, pp. 2219-2225.

[8] D. Rodrigo, B. A. Cetiner, and L. Jofre, "Frequency, radiation pattern and polarization reconfigurable antenna using a parasitic pixel layer," *IEEE Trans. Ant. Propagat.*, vol. 62, Jun 2014, pp. 3422-3427.

[9] S. Song and R. D. Murch, "An Efficient Approach for Optimizing Frequency Reconfigurable Pixel Antennas Using Genetic Algorithms," *IEEE Trans. Ant. Propagat.*, vol. 62, Feb 2014, pp. 609-620.

[10] A. Grau, M.-J. Lee, J. Romeu, H. Jafarkhani, L. Jofre, and F. De Flaviis, "A Multifunctional MEMS-Reconfigurable Pixel Antenna for Narrowband MIMO Communications," *IEEE APS International Symposium*, 2007, pp. 489-492.

[11] A. Grau and F. De Flaviis, "A Distributed Antenna Tuning Unit Using a Frequency Reconfigurable PIXEL-Antenna," *Proc. EuCAP*, 4th, 2010, pp. 1-5.

[12] N. Haider, D. Caratelli, and A. G. Yarovoy, "Recent Developments in Reconfigurable and Multiband Antenna Technology," *IJAP, Hindawi Pub. Corp.*, 2013, pp. 1-14.

[13] Alfred Grau, Jordi Romeu, Lluis Jofre, and Franco De Flaviis, "A Software Defined MEMS-Reconfigurable PIXEL-Antenna for Narrowband MIMO Systems," *NASA/ESA Conference on Adaptive Hardware and Systems*, 2008, pp. 141-146.

[14] E. Y. Lee, E. K. Walton, J. Young, S. Gemeny, D. Crowe, and C. Harton, "The Software Defined Antenna: Measurement and Simulation of a 2 Element Array," *IEEE APSIS, APSURSI'09*, Charleston, SC, 1-5 Jun 2009, pp. 1-4.

[15] E. Y. Lee, E. K.Walton, J. Young, S. Gemeny, T.-H. Lee, N. Roberts, E. Bosso, and E. Huang, "The Software Defined Antenna: Microstrip Antennas with Gaps," *IEEE APSIS, APSURSI'10*, Toronto, ON, 11-17 Jul 2010, pp. 1-4.

[16] E. Y. Lee, S. Gemeny, E. Walton, T.-H. Lee, D. Devoe, P. Haresh, and J. Felder, "The Software Defined Antenna; MEMS based pixel prototyping," *Antenna Measurement Techniques Association (AMTA), 25th Annual Meeting and Sympos.*, Oct 2013, pp. 187-190.

[17] J. Kovitz and Y. Rahmat-Samii, "Micro-actuated pixel patch antenna design using particle swarm optimization," *IEEE International Symposium on Antennas and Propagation (APSURSI)*, pp. 2415-2418 July 2011.

[18] D. Rodrigo, "Real-Time Reconfigurable Pixelled Antennas," M.Sc thesis, Department of Signal Theory and Communications, University of Catalunya, July 2010.

[19] D. Rodrigo, "Frequency and radiation pattern reconfigurability of a multi-size pixel antenna," *IEEE Transactions on Antennas and Propagation*, Vol. 60, pp. 2219-2225, May 2011.

[20] D. Rodrigo, "Interference rejection using frequency and pattern reconfigurable antennas," *IEEE Antennas and Propagation Society International Symposium*, pp. 1-2, July 2012.

[21] X. Yuan, Z. Li, D. Rodrigo, H. S. Mopidevi, O. Kaynar, L. Jofre, and B. A. Cetiner, "A Parasitic Layer-Based Reconfigurable Antenna Design by Multi-Objective Optimization," *IEEE Trans. Ant. Propagat.*, vol. 60, Jun 2012, pp. 2690-2701.

[22] X. Yuan, "Multifunctional reconfigurable antenna development by multi-objective optimization," PhD thesis, Department of Electrical and Computer Engineering, Utah State University, Logan, Utah, 2012.

[23] Daniel Rodrigo, "Reconfigurable Pixel Antennas for Communications," PhD thesis, Department of Signal Theory and Communications, University of Catalunya, April 2013.

[24] Advanced Design System 2011, Help Center, Agilent® Technologies.

[25] J. Panda and R. Kshetrimayum, "Parametric Study of Printed Rectangular Monopole Antennas," *International Journal of Recent Trends in Engineering.*, vol. 1, pp. 42–46, May 2009.

[26] G. Kumar, *Broadband Microstrip Antennas*, Artech House, Inc., 2003.